THE JOURNAL OF BIOLOGICAL CHEMISTRY VOL. 287, NO. 13, pp. 9901–9909, March 23, 2012

Mutations in N-terminal Flanking Region of Blue Light-sensing Light-Oxygen and Voltage 2 (LOV2) Domain Disrupt Its Repressive Activity on Kinase Domain in the *Chlamydomonas* Phototropin*[S]

Received for publication, November 16, 2011, and in revised form, January 26, 2012 Published, JBC Papers in Press, January 30, 2012, DOI 10.1074/jbc.M111.324723

Yusuke Aihara[‡], Takaharu Yamamoto[§], Koji Okajima[¶], Kazuhiko Yamamoto[‡], Tomomi Suzuki[‡], Satoru Tokutomi[¶], Kazuma Tanaka[§], and Akira Nagatani[‡1]

From the [‡]Department of Botany, Graduate School of Science, Kyoto University, Kyoto 606-8502, Japan, the [§]Division of Molecular Interaction, Institute for Genetic Medicine, Hokkaido University Graduate School of Life Science, Sapporo 060-0815, Japan, and the [¶]Department of Biological Sciences, Graduate School of Science, Osaka Prefecture University, Osaka 599-8531, Japan

Background: A plant photoreceptor "phototropin" is a light-dependent kinase containing the LOV photosensory domains.
Results: Mutations in the N-terminal flanking region of LOV2 elevate kinase activity in darkness.
Conclusion: The N-terminal flanking region is involved in intramolecular signaling from LOV2 to the kinase domain.
Significance: This work provides insights into how the LOV domain can activate the kinase domain intramolecularly.

Phototropin is a light-regulated kinase that mediates a variety of photoresponses such as phototropism, chloroplast positioning, and stomata opening in plants to increase the photosynthetic efficiency. Blue light stimulus first induces local conformational changes in the chromophore-bearing light-oxygen and voltage 2 (LOV2) domain of phototropin, which in turn activates the serine/threonine (Ser/Thr) kinase domain in the C terminus. To examine the kinase activity of full-length phototropin conventionally, we employed the budding yeast *Saccharomyces cerevisiae*. In this organism, Ser/Thr kinases (Fpk1p and Fpk2p) that show high sequence similarity to the kinase domain of phototropins exist. First, we demonstrated that the phototropin from *Chlamydomonas reinhardtii* (*Cr*PHOT) could complement loss of Fpk1p and Fpk2p to allow cell growth in yeast. Furthermore, this reaction was blue light-dependent, indicating that *Cr*PHOT was indeed light-activated in yeast cells. We applied this system to a large scale screening for amino acid substitutions in *Cr*PHOT that elevated the kinase activity in darkness. Consequently, we identified a cluster of mutations located in the N-terminal flanking region of LOV2 (R199C, L202L, D203N/G/V, L204P, T207I, and R210H). An *in vitro* phosphorylation assay confirmed that these mutations substantially reduced the repressive activity of LOV2 on the kinase domain in darkness. Furthermore, biochemical analyses of the representative T207I mutant demonstrated that the mutation affected neither spectral nor multimerization properties of *Cr*PHOT. Hence, the N-terminal flanking region of LOV2, as is the case with the C-terminal flanking Jα region, appears to play a crucial role in the regulation of kinase activity in phototropin.

To sense and respond to a fluctuating light environment, plants have evolved several classes of photoreceptor molecules that convert visible light stimuli into biological signals. Phototropin (PHOT)[2] is a blue light (BL) receptor, which is widely conserved in the plant kingdom (1). Most terrestrial plants possess two isoforms of phototropin designated PHOT1 and PHOT2. In *Arabidopsis thaliana* (*At*), PHOT1 and PHOT2 have redundant and distinct functions to mediate responses, such as phototropism (2, 3), chloroplast movement (4, 5), stomatal opening (6), and leaf photomorphogenesis (7, 8) to optimize photosynthesis. On the other hand, the unicellular green alga *Chlamydomonas reinhardtii* (*Cr*) possesses a single phototropin homologue (*Cr*PHOT), which has been proposed to regulate sexual differentiation (9, 10) and the expression several photosynthetic genes. Interestingly, *Cr*PHOT is fully functional in *Arabidopsis*, suggesting that the basic mechanism of phototropin signal transduction is highly conserved (11). Phototropins are BL-dependent Ser/Thr protein kinases that share well conserved structural properties. The kinase domain belongs to the AGC VIII subfamily (protein kinases A, G, and C) (12). Autophosphorylation of a conserved serine residue at the activation loop of the kinase domain is prerequisite for its physiological activity (13, 14). To date, little is known about authentic phosphorylation substrates for phototropins. Recently, however, auxin efflux transporter ATP-binding cassette B19 (ABCB19) has been reported as a putative endogenous substrate in *Arabidopsis* (15).

* This work was supported Grant-in-aid for Scientific Research on Priority Areas 17084002 (to A. N.), Grant-in-aid for Scientific Research on Innovative Areas 22120002 (to A. N.), a Grant-in-aid for the Global COE (Center of Excellence) Program "Formation of a Strategic Base for Biodiversity and Evolutionary Research: From Genome to Ecosystem" (to A. N.) from the Ministry of Education, Culture, Sports, Science, and Technology, Japan, Grant-in-aid for Scientific Research (B) 21370020 (to A. N.), and Research Fellowship 22.1094 from the Japan Society for the Promotion of Science (to Y. A.).

[S] This article contains supplemental Figs. S1–S7.

[1] To whom correspondence should be addressed. Tel.: 81-75-753-4123; Fax: 81-75-753-4126; E-mail: nagatani@physiol.bot.kyoto-u.ac.jp.

[2] The abbreviations used are: PHOT, phototropin; *At*P1-Nt; N-terminal fragment of *Arabidopsis* PHOT1; BL, blue light; CBB, Coomassie Brilliant Blue; *Cr*PHOT, *Chlamydomonas* phototropin; Fpk1p, flippase-kinase 1; LOV, light-oxygen and voltage.

In addition to the kinase domain, phototropin contains two N-terminal light-oxygen and voltage (LOV) domains, designated LOV1 and LOV2. The LOV domains, which are members of the Per-ARNT-Sim (PAS) domain superfamily, noncovalently bind flavin mononucleotide (FMN) as chromophores (16). Because the kinase fragment lacking LOV domains displays constitutive activity both *in planta* (17) and *in vitro* (18), LOV domains appear to suppress kinase activity in darkness intrinsically.

Upon BL absorption, a covalent adduct is formed between the FMN and a conserved cysteine residue within each LOV domain (19, 20). Consequently, reorganization of the hydrogen bond network takes place in the FMN binding pocket (21, 22). Inactivation of LOV domains by site-directed mutagenesis indicates that LOV2 plays a predominant role in regulating the kinase activity (18, 23, 24), whereas the role of LOV1 is limited to modulate photosensitivity (18). An NMR analysis of *Avena* PHOT1 has revealed an amphipathic α helix, Jα, which is attached to the C terminus of the LOV2 core domain (25). The Jα helix changes its structure in response to a light stimulus. Namely, it detaches from the LOV2 core (25) and unfolds (26, 27). The prominent role of the Jα helix in the regulation of kinase activity has been evidenced by site-directed mutagenesis in *Arabidopsis* PHOT1. An amino acid substitution that disrupts the LOV2-Jα interaction leads to constitutive activation of the kinase *in vitro* (28). More recently, the crystallographic analysis of *Avena* PHOT1 LOV2 has suggested that not only the C-terminal Jα but also the N-terminal flanking region display a light-induced structural change (22). These structural changes are presumed to disrupt the inhibitory interaction of LOV2 with the kinase domains. Accordingly, photoreversible contact/separation between the LOV2 and the kinase domains has been suggested by small angle x-ray scattering in a LOV2 linker kinase fragment of *Arabidopsis* PHOT2 (29).

Besides the site-directed mutagenesis approach based on structural information, a random-mutagenesis approach utilizing *Escherichia coli* as a host has been applied successfully to uncover amino acid residues involved in the photochemistry of LOV2 in *Avena* PHOT1 (30). Although this method is quite effective for identifying spectral mutants in the LOV domains, it is not applicable for screening mutants that are altered in the photoregulation of the kinase activity. This is because no convenient way to assess the kinase activity of phototropin exists in *E. coli*.

In this study, we developed a new yeast experimental system in which *Cr*PHOT triggered cell growth depending on its kinase activity. We applied this method to screen for mutations that disrupt repression of the kinase domain. Consequently, we revealed that the N-terminal flanking region of LOV2 is important for the suppression of kinase activity in darkness.

EXPERIMENTAL PROCEDURES

Media and Growth Conditions for Yeast—Yeast strains were cultured in YPDA-rich medium (1% yeast extract, 2% bactopeptone, 2% glucose, and 0.01% adenine). Strains carrying plasmids were selected in synthetic medium (SD) containing the required nutritional supplements (31). When appropriate, 0.5% casamino acids were added to SD medium without uracil (SDA-Ura). For induction of the *GAL1* promoter, 3% galactose and 0.2% sucrose were added as carbon sources instead of glucose (YPGA and SGA-Ura). Growth sensitivity to duramycin was examined on YPDA plates containing 10 μM duramycin (Sigma). Blue (peak at 470 nm) and red (peak at 660 nm) light-emitting diode panels (ISL-150X150 series; CCS, Tokyo, Japan) were used as light sources.

Strains and Plasmids—*Saccharomyces cerevisiae* strains KKT330 (MATa *ura3*Δ *his3*Δ*1 leu2*Δ*0 HIS3MX6::*P_{GAL1}*-CDC50 fpk1*Δ*::HphMX4 fpk2*Δ*::KanMX6*, designated hereafter as P_{GAL1}*-CDC50 fpk1*Δ *fpk2*Δ) and YKT1638 (MATa *ura3*Δ *his3*Δ*1 leu2*Δ*0 fpk1*Δ*::HphMX4 fpk2*Δ*::KanMX6,* designated hereafter as *fpk1*Δ *fpk2*Δ) were used for growth assays (32). The *E. coli* strains DH5α and BL21 were used for plasmid construction and expression of recombinant proteins, respectively.

For yeast assays, pRS416-AtPHOT1, pRS416-AtPHOT2, and pRS416-CrPHOT were constructed as follows. The coding regions of *PHOT1* and *PHOT2* from *Arabidopsis* and *PHOT* from *Chlamydomonas* were amplified by PCR and cloned into the BamI/SalI site of pRS416 (33) to allow constitutive expression of phototropins tagged with N-terminal two tandem repeats of the influenza virus hemagglutinin epitope (2HA) under the control of the *TPI1* promoter. Site-directed mutations were introduced by using the QuikChange site-directed mutagenesis kit (Stratagene) in accordance with the instructions of the supplier. All amino acid changes were verified by DNA sequencing. For overexpression of *Cr*PHOT protein in *E. coli*, pET28a-CrPHOT was constructed as follows. Wild-type (WT) and mutant *PHOT* were amplified from pRS416-CrPHOT and cloned into NdeI/SalI sites of pET28a plasmid vector (Novagen) to allow expression of *Cr*PHOT with an N-terminal histidine tag, which was composed of 20 residues including six histidine residues.

Immunoblot Analysis—Protein extraction from yeast was performed as described (34). Immunoblot analysis was performed essentially as described previously (11). The same amounts of protein extracts were run on 10.0% SDS-PAGE and blotted onto nitrocellulose membrane. Rat anti-HA monoclonal antibody (Roche Applied Science) and alkaline phosphatase-conjugated anti-rat IgG antibody (Promega) were used.

Yeast Growth Assay—The cells were grown in liquid SGA-Ura medium to A_{600} of 0.6–0.8, harvested by centrifugation, and resuspended into sterile water, resulting in an A_{600} of 0.1. Serial 5-time dilutions were then prepared for loading 10 μl each of the diluted cell suspension onto a plate with SGA-Ura or SDA-Ura medium. The plates were then placed under different light conditions.

PCR-based Random Mutagenesis and Mutant Screening for Pseudolit Phenotype—Error-prone PCR libraries of the N-terminal (1–1399) and C-terminal (1179–2136) moieties of *Cr*PHOT flanked by sequences from the pRS416 vector (~150 bp) were generated from the pRS416-CrPHOT using the Diversity PCR random mutagenesis kit (Clontech). The primer sequences are as follows: pRS416 forward for the N-terminal library, 5′-GTGAACTTGCAACATTTACTATTTTCCC; CrPHOT-1399 reverse for the N-terminal library, 5′-CGGTCTGGATGGTGCAGTACAG; CrPHOT-1179 forward for the C-terminal library, 5′-CTACCAGGCGCTGCTGCAGCTG;

and pRS416 reverse for the C-terminal library, 5′-AAAGCGG-GCAGTGAGCGCAACGC. Final concentrations of 320 μM $MnSO_4$ and 16 μM dGTP were chosen for the PCR to adjust the mutagenesis frequency to 1.5 mutations/kb.

The pRS416-CrPHOT plasmid was digested with BamHI/NruI and SalI/NruI to remove the sequence encoding the N-terminal and C-terminal moieties, respectively. The N- or C-terminal PCR fragments and a pRS416-CrPHOT-derived vector lacking the corresponding part of *Cr*PHOT were mixed and transformed into the P_{GAL1}-*CDC50 fpk1*Δ *fpk2*Δ yeast strain, so that homologous recombination generated a vector containing mutagenized *PHOT*. The yeast strain was then plated on SDA-Ura agar and incubated in the dark at 28 °C for 60 h. The growing colonies were isolated. Among isolated colonies, candidates were randomly selected, and plasmids were rescued using Wizard prep (Promega) according to the instructions in the DUALhybrid kit (Dualsystems Biotech). The candidate plasmids were sequenced in the mutagenized moieties. The second growth assay was performed by repeating the assays using the purified plasmids.

Expression and Purification of Recombinant Proteins—His_6-tagged full-length *Cr*PHOT and N-terminal fragment of *Arabidopsis* PHOT1 (*At*P1-Nt) were prepared from *E. coli* according to the protocols used for LOV2 linker kinase fragment preparation (35) with minor modifications. The *E. coli* cells were lysed with a French pressure cell (Thermo Fisher Scientific) in a buffer containing 20 mM HEPES-NaOH (pH 7.8), 500 mM NaCl, and 1 mM PMSF. The purification was performed at 0–4 °C under a dim red light. The centrifugation supernatant of the lysate was subjected to Ni^{2+}-ion affinity chromatography (Qiagen). The *At*P1-Nt were then desalted by using HiTrap Desalting (GE Healthcare) and stored at −80 °C.

The *Cr*PHOT protein was further purified via size-exclusion column chromatography (Sephacryl HR 200; GE Healthcare) in a buffer containing 100 mM NaCl, 1 mM EGTA, and 20 mM Tris-HCl (pH 7.8). Glycerol was added to the eluted *Cr*PHOT to a final concentration of 10% (v/v). The phosphorylation levels of the products after purification were examined by Pro-Q Diamond phosphoprotein gel stain (Invitrogen) according to the manufacturer's instructions if necessary.

For the spectral analysis, the above sample was further purified using an anion-exchange Resource Q column (GE Healthcare) equilibrated with a buffer containing 10% (v/v) glycerol, 1 mM EGTA, and 20 mM Tris-HCl (pH 7.8). The *Cr*PHOT fraction that did not bind to the Resource Q column was collected and concentrated by ultrafiltration using the Amicon Ultra K15 (Millipore). The purity of *Cr*PHOT in each step was examined by SDS-PAGE.

In Vitro Phosphorylation Assays—The phosphorylation assay was performed under dim green light (18, 35). *Cr*PHOT and *At*P1-Nt polypeptides were incubated at 30 °C in a kinase reaction mixture containing 20 mM Tris-HCl (pH 7.8), 100 mM NaCl, 10% glycerol, 10 mM MgCl, 500 μM ATP, and 60 kBq of [γ-^{32}P]ATP. The reaction was terminated by the addition of concentrated SDS-PAGE sample buffer followed by boiling for 3 min. Then, the samples were run on SDS-PAGE to visualize phosphorylation bands using an imaging plate and a bioimaging analyzer (FLA2000; Fuji, Tokyo, Japan). The molecular masses of phosphorylated proteins were estimated by Coomassie Brilliant Blue (CBB) staining with reference to molecular mass standard samples (Sigma).

Spectral Analyses and Size-exclusion Chromatography—The absorption spectra of *Cr*PHOT under BL illumination and the time course of absorption changes during thermal decay from the cysteinyl adduct state to the dark-adapted state were measured essentially as described previously (35) at 20 °C and pH 7.8. The molecular mass of *Cr*PHOT was estimated by size-exclusion chromatography using a Superdex 200 pg Hi-Load column (GE Healthcare) and the kinase reaction buffer as previously described (35).

RESULTS

*Complementation of fpk1*Δ *fpk2*Δ *and cdc50*Δ *Synthetic Lethality in S. cerevisiae by Chlamydomonas PHOT in a BL-dependent Manner*—To establish an experimental system that can easily and quickly assess the light-dependent kinase activity of phototropin, we employed *S. cerevisiae*, in which the protein kinases named flippase-kinase 1 (Fpk1p) and Fpk2p were recently identified (32). Among the yeast kinases, Fpk1p and Fpk2p exhibit the highest sequence homology to the AGCVIII kinase domain of phototropins (32) (Fig. 1*A* and supplemental Fig. S1). Hence, we reasoned that phototropins might complement the loss of *FPK*s in yeast in a light-dependent manner.

FPK1 and *FPK2* exhibit synthetic growth defects with the null mutation of *CDC50* (36, 37). Their products, Fpk1p and Fpk2p, regulate the Lem3p-Dnf1p and Lem3p-Dnf2p flippases, which act as inward-directed phospholipid translocases (38). Nakano *et al.* have established a conditional mutant in which Cdc50p is expressed under the control of the glucose-repressible *GAL1* promoter in the *fpk1*Δ *fpk2*Δ background (P_{GAL1}-*CDC50 fpk1*Δ *fpk2*Δ) (32). The resultant P_{GAL1}-*CDC50 fpk1*Δ *fpk2*Δ mutant grows normally in galactose-containing medium (SGA-Ura) but exhibits severe growth defect in glucose-containing medium (SDA-Ura) (Fig. 1*B*) (32). To examine whether phototropins could rescue the loss of *FPKs* in yeast, we introduced the *Arabidopsis PHOT1* (*AtPHOT1*) and *PHOT2* (*AtPHOT2*), and *Chlamydomonas PHOT* (*CrPHOT*) genes into the P_{GAL1}-*CDC50 fpk1*Δ *fpk2*Δ strain. Consequently, *AtPHOT2* partly suppressed the growth defect in glucose-containing medium regardless of the light condition, whereas *AtPHOT1* completely failed to allow growth (supplemental Fig. S2). Remarkably, *CrPHOT*, albeit partially, suppressed the growth defect under BL but not in darkness (Fig. 1*B*) or under red light (Fig. 1*D*). Thus, *Cr*PHOT complemented the loss of Fpk activity in a BL-dependent manner in yeast.

CrPHOT Acts as a Light-dependent Flippase-Kinase in Yeast—We genetically examined whether the kinase activity of *Cr*PHOT was indeed required for the complementation. The kinase domain fragments of phototropins exhibit constitutive kinase activity without light stimulus (17, 18). As expected, the kinase domain fragment of *Cr*PHOT restored yeast growth regardless of the light condition (Fig. 1*B*). Conversely, the D549N mutant of *Cr*PHOT, which corresponded to the kinase-dead mutation in *At*PHOT1 and *At*PHOT2 (17, 23), failed to restore growth. The substitution of conserved Cys^{39} to alanine in the LOV2 domain is known to decrease the extent of light

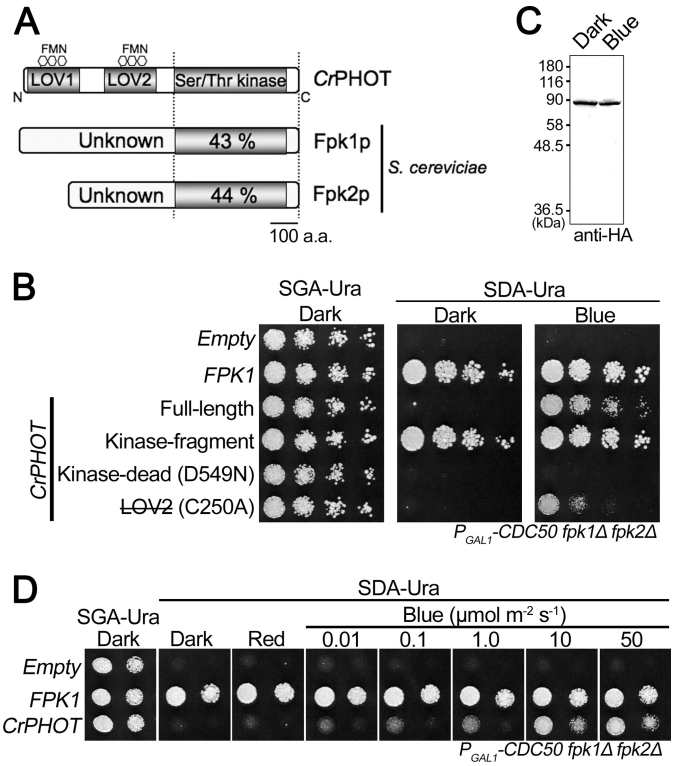

FIGURE 1. **Photoregulation of yeast cell growth by *Cr*PHOT.** The yeast conditional mutant P_{GAL1}-*CDC50 fpk1*Δ *fpk2*Δ was transformed with a vector containing the *FPK1* gene or *CrPHOT* derivatives fused to the constitutive *TPI1* promoter. *A*, schematic illustration of the phototropin from *Cr*PHOT and Fpk1p and Fpk2p from *S. cerevisiae*. The *numbers* within the Ser/Thr kinase domain show the percentage sequence identity with the *Cr*PHOT kinase domain. *B*, growth of the yeast conditional mutant P_{GAL1}-*CDC50 fpk1*Δ *fpk2*Δ expressing the full-length *CrPHOT* and its derivatives. *LOV2* (with a line through it) *Cr*PHOT with a mutation that decreases the extent of light activation. Yeast cells were serially diluted and spotted onto plates containing galactose (SGA-Ura) or glucose (SDA-Ura), followed by incubation in darkness (*Dark*) or under BL irradiation (50 μmol m^{-2} s^{-1}; *Blue*) at 28 °C for 2–3 days. *Empty*, yeast cells transformed with a control plasmid. *C*, immunoblot detection of the full-length *Cr*PHOT with an anti-HA monoclonal antibody in yeast grown as for *B*. Protein extracts from 1 mg of wet yeast cells were separated by 10.0% SDS-PAGE. *D*, effects of monochromatic light irradiation on growth of yeast expressing *CrPHOT*. Red light at 50 μmol m^{-2} s^{-1} or blue light at different intensities was applied to yeast cells as for *B*.

activation in phototropins (18, 23). The corresponding C250A mutant of *Cr*PHOT restored growth but very weakly (Fig. 1*B*). Taken together, *Cr*PHOT complemented the loss of Fpks in a kinase-like manner.

We then examined whether the complementation by *Cr*PHOT indeed depended on its light activation. First, we confirmed that the level of *Cr*PHOT in yeast was not altered under BL with an anti-HA tag antibody (Fig. 1*C*). This was because phototropin is known to be degraded more rapidly under BL in some cases (7, 39). It should be noted that electric mobility shift due to BL-induced autophosphorylation was not observed. This was probably because such activity is low in *Cr*PHOT (11).

We determined the dependence of complementation by *Cr*PHOT on BL intensity (Fig. 1*D*). The degree of complementation increased as BL was increased from 0.01 to 10 μmol m^{-2} s^{-1}. This result matched well with those from a previous analysis on the biological activity of *Cr*PHOT expressed in *Arabidopsis* (11).

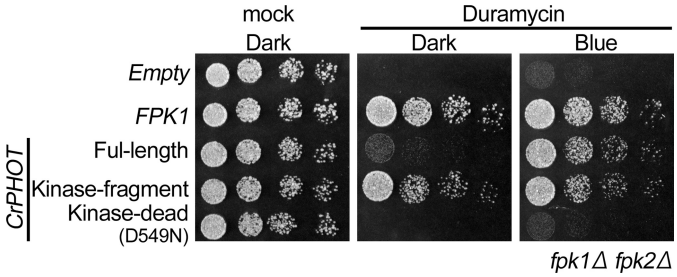

FIGURE 2. **Growth sensitivity to duramycin of the *fpk1*Δ *fpk2*Δ mutant expressing *CrPHOT* and its derivatives.** The yeast cells were serially diluted and spotted onto YPDA plates with or without 10 μM duramycin. The plates were then incubated in darkness (*Dark*) or under BL irradiation (50 μmol m^{-2} s^{-1}; *Blue*) at 28 °C for 1.5 days.

BL-dependent Regulation of Phospholipid Uptake by CrPHOT—We further examined whether *Cr*PHOT activated flippases in yeast as Fpks do. Phosphatidylethanolamine is enriched in the outer leaflet of the membrane in *fpk1*Δ *fpk2*Δ mutant due to reduced flippase activity. This leads to growth defect in the presence of duramycin, a cytotoxic small tetracyclic peptide that binds phosphatidylethanolamine on the outer leaflet. As expected, *Cr*PHOT rescued the duramycin-sensitive growth defect in a BL-dependent manner (Fig. 2). In addition, the kinase fragment rescued the phenotype regardless of the light condition, whereas the putative kinase-dead mutant (D549N) of *Cr*PHOT failed to restore the growth. Hence, *Cr*PHOT was suggested to regulate the flippase activity in yeast.

Search for Novel CrPHOT Variants Showing Pseudolit Activity—The above experimental system should be potentially useful in identifying amino acid residues important for phototropin functions. To explore this possibility, mutations were introduced separately into the N- and C-terminal moieties of *CrPHOT* by a PCR-based method at the rate of 1.5 mutations/kb (Fig. 3*A*). Pools of transformed cells corresponding to 5.0×10^5 each of successful recombination events were screened for mutations that allowed growth in darkness on SDA-Ura plates. Consequently, 1504 and 107 growth-positive colonies were obtained for the N- and C-terminal mutant pools, respectively.

We then sequenced 96 randomly selected clones for the N-terminal mutations and all 107 clones for the C-terminal mutations. Consequently, we found that many of them carried multiple amino acid substitutions. In addition, a large deletion, probably due to irregular homologous recombination, was found in some clones. Nonetheless, eight clones with single amino acid substitutions were identified (Fig. 3*A*). Additionally, four substitutions were shared in more than three independent clones with multiple mutations. Reintroduction of the latter mutations into the wild-type *CrPHOT* confirmed that they indeed conferred the pseudolit phenotype (Fig. 3*C* and supplemental Fig. S3). We also confirmed that the expression levels of these mutant proteins were not elevated in yeast cells (supplemental Fig. S4).

Kinase Activities of Full-length CrPHOT Carrying Mutations in the N-terminal Flanking Region of LOV2—Interestingly, 8 of the above 12 mutations were clustered in a well conserved N-terminal LOV2-flanking region (residues Arg^{199}-Arg^{210}) (Fig. 3, *A* and *B*). Hence, their kinase activity was examined *in*

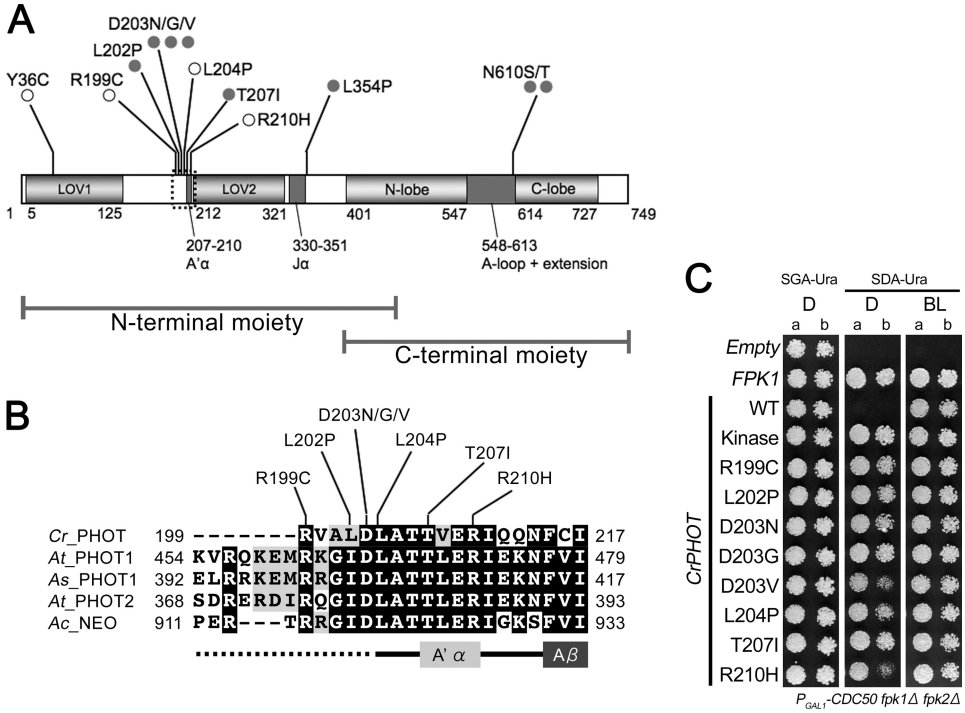

FIGURE 3. ***CrPHOT* mutants that restored yeast growth in darkness.** *A*, schematic drawing of the domain structure of *Cr*PHOT and locations of amino acid substitutions found in the present studies. *Gray filled circles* indicate mutations identified in clones with a single mutation. *Open circles* indicate mutations found in more than three independent clones with multiple mutations. *B*, sequence alignment of N-terminal flanking regions of LOV2 among different phototropin species. *Cr*_PHOT, *C. reinhardtii* PHOT; *At*_PHOT1, *A. thaliana* PHOT1; *As*_PHOT1, *Avena sativa* PHOT1; and *At*_PHOT2, *A. thaliana* PHOT2; *Ac*_NEO, *Adiantum capillus-veneris* NEOCHROME1. Sequences were aligned using the ClustalW and BOXSHADE program. *C*, growth of the P_{GAL1}-*CDC50 fpk1*Δ *fpk2*Δ mutant expressing *CrPHOT* with single amino acid substitutions. Cells were treated as for Fig. 1*B*. Two concentrations of yeast cells (*a*, $A_{600} = 0.004$; *b*, $A_{600} = 0.0008$) were spotted.

vitro. For this purpose, we attempted to express the recombinant full-length *Cr*PHOT protein tagged with an N-terminal His_6 tag in *E. coli*. Full-length *Cr*PHOT protein was recovered as a yellow-colored, soluble protein from the *E. coli* extract. For the kinase assay, the *Cr*PHOT protein was purified from the extract by Ni^{2+}-affinity chromatography and size-exclusion chromatography. SDS-PAGE revealed that the resulting sample consisted of a main band of 90 kDa, which corresponded to the theoretical mass of the protein, 85.7 kDa, with several minor bands of lower molecular masses. The purity was then estimated to be ~75% (Fig. 4*A*), which was comparable with those of samples used for the previous kinase assays of LOV kinase fragments (18, 35).

In vitro phosphorylation assay for the purified *Cr*PHOT was performed using *At*P1-Nt as a substrate (35). As expected, *Cr*PHOT phosphorylated *At*P1-Nt under BL, whereas phosphorylation was substantially reduced in darkness (Fig. 4*B*). The phosphorylation level increased during the incubation period of 60 min. The effects of BL were saturated at ~10 μmol m^{-2} s^{-1} (Fig. 4*C*). It should be noted that the background activity in darkness was relatively high, which has been reported for other phototropin samples as well (40, 41).

We then examined the kinase activities in 6 of 8 mutants carrying the mutation in the N-terminal flanking region of LOV2 (R199C, D203N, L204P, T207I, and R210H). The full-length proteins were expressed in *E. coli* and purified as described above. Consequently, protein samples in similar qualities were obtained with the exception of R199C in which a larger amount of impurity at around 36.5 kDa was detected (Fig. 5*A*).

We examined the kinase activity using *At*P1-Nt as a substrate. Consistent with the yeast phenotype (Fig. 3), the above mutants exhibited increased kinase activities in darkness compared with the WT with the exception of D203N (Fig. 5, *B* and *C*). Hence, most of the *Cr*PHOT mutants disrupted repression of the kinase activity *in vitro*.

Spectroscopic Analysis of Mutation in N-terminal Flanking Region of LOV2—We examined whether the present mutations affected the spectral nature of *Cr*PHOT. For this purpose, the T207I mutant was selected as a representative mutant and expressed in *E. coli*. The protein sample conventionally prepared according to the procedure listed for the kinase assay was further purified by negative ion exchange chromatography. Consequently, a sample with >95% purity was obtained (Fig. 6*A*). The absorption spectroscopy revealed that both WT and T207I mutant exhibited the typical fine structured absorption spectra of protein-bound FMN with absorption maxima at 425, 447, and 472 nm (Fig. 6*B*). Under continuous BL irradiation, both WT and T207I *Cr*PHOT proteins were converted to cysteinyl adduct state with absorption maxima at 390 nm (Fig. 6*B*). Those absorption spectra were nearly identical to those of the LOV1-hinge-LOV2 fragment of *Cr*PHOT, which lacked the kinase domain (42).

At a fluence rate of 270 μmol m^{-2} s^{-1}, adduct formation was saturated within 24 s, whereas the dark reversion was completed within 400 s after the illumination was turned off (data

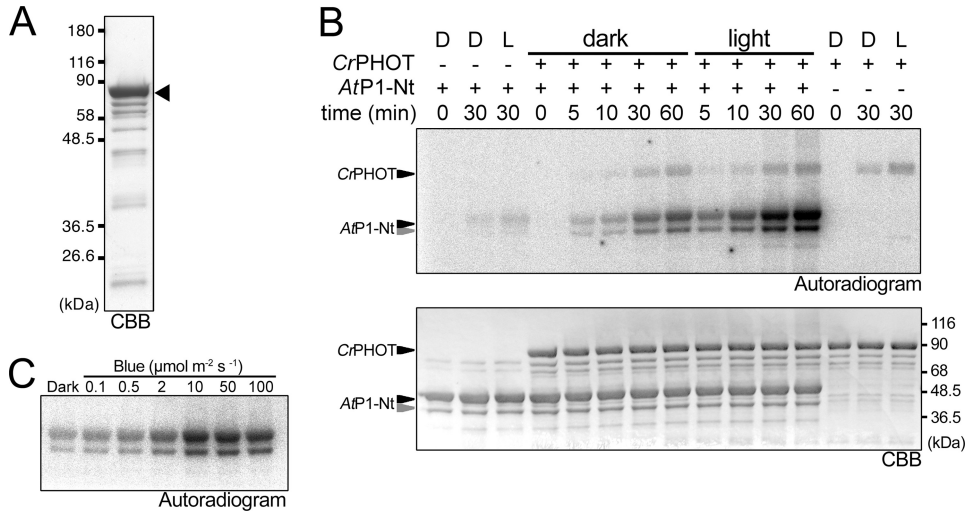

FIGURE 4. ***In vitro* phosphorylation assay of the full-length *Cr*PHOT.** *A*, 10.0% SDS-polyacrylamide gel pattern of full-length *Cr*PHOT stained with CBB. The sample with an N-terminal His_6 tag was successively purified by Ni^{2+}-ion affinity chromatography and size-exclusion chromatography. The *triangle* indicates the position of the intact *Cr*PHOT. *B*, *in vitro* phosphorylation assay for *Cr*PHOT under BL (100 μmol m^{-2} s^{-1}) or in the dark. *Cr*PHOT and/or *At*P1-Nt was incubated with radioactive ATP for the indicated durations. The *upper* and *lower panels* show the 10.0% SDS-PAGE gel patterns visualized by autoradiography and CBB staining, respectively. + or −, the presence or absence of the kinase and/or the substrate, respectively; *D*, dark condition; *L*, BL irradiation. *C*, dependence of the kinase activation on the light intensity. *In vitro* phosphorylation assay of *Cr*PHOT was performed as described for *B*. The samples were incubated for 10 min under BL at the indicated light intensities. Phosphorylated *At*P1-Nt was visualized by autoradiography.

not shown). By exponential fitting analysis, the half-lives for dark decay of two photoproduct components in WT *Cr*PHOT were calculated to be 15 and 50 s, whereas those for the T207I mutant were 15 and 56 s. Hence, the T207I mutant was almost indistinguishable from the WT. Taken together, the T207I mutation in the N-terminal flanking region of LOV2 activated the kinase domain without affecting the spectral nature of *Cr*PHOT.

Estimation of Molecular Mass by Size-exclusion Chromatography—LOV1 domains in phototropins have been suggested to form a dimer (43–45). Hence, we examined the possibility that the T207I mutation affected kinase activity by altering the multimerization state of full-length *Cr*PHOT. To test this possibility, we determined the molecular masses of full-length WT and T207I *Cr*PHOT by size-exclusion chromatography. For this purpose, the samples were purified as for the spectral analysis.

The size-exclusion elution profile demonstrated that both WT and T207I *Cr*PHOT proteins exhibited a major distinct peak at 71.14 ml, corresponding to a molecular mass of 123.7 kDa (supplemental Fig. S5). Hence, the T207I mutation did not alter the multimerization state of full-length *Cr*PHOT. Another minor peak at 78 ml (corresponding to 68 kDa) probably represented a degradation product.

DISCUSSION

CrPHOT Complements Loss of Fpk1p and Fpk2p Kinases in Yeast—A bacterial system has been employed successfully to identify amino acid residues important for the spectral integrity of the LOV domains of phototropins (30). The present study further extended this strategy to assess the signaling activity of phototropin derivatives in a microorganism.

Indeed, *Cr*PHOT successfully rescued the *fpk1*Δ *fpk2*Δ phenotype to allow cell growth in a BL-dependent manner in yeast (Fig. 1). We further demonstrated that both photoexcitation of the LOV domain and the kinase activity of *Cr*PHOT are necessary to promote yeast cell growth (Fig. 1*B*). Hence, we have developed an experimental system suitable for a large scale mutant screening for *Cr*PHOT.

It remains unclear why the *Arabiodopsis PHOT1* and *PHOT2* did not function properly in yeast. To gain further insights, the complementation activities of respective kinase fragments were examined. Consequently, the PHOT1 kinase fragment failed to promote the cell growth, whereas the PHOT2 fragment did (supplemental Fig. S2). Hence, intrinsic kinase activities of *Arabiodopsis* PHOT1 and PHOT2 appeared to be quite different in yeast for an unknown reason.

Kinase Activity of Full-length CrPHOT—It had long been believed that expression of recombinant full-length phototropins in *E. coli* for biochemical analyses was very difficult. Recently, however, Pfeifer *et al.* successfully purified full-length *Cr*PHOT in *E. coli* to conduct FTIR spectroscopy (46). Similarly, we were able to prepare full-length WT and mutated *Cr*PHOT proteins pure enough for the *in vitro* kinase assay, photochemical kinetic analysis, and multimerization analysis.

The BL-dependent kinase activity of the purified *Cr*PHOT was successfully shown *in vitro* using *At*P1-Nt as a substrate (Fig. 4*B*). As has been shown already for *Cr*PHOT expressed in insect cells (11), autophosphorylation activity was relatively low. This was not because the purified *Cr*PHOT was already phosphorylated in *E. coli* (supplemental Fig. S6). We suppose that fewer phosphorylation sites exist in *Cr*PHOT (11).

Spectral and Multimerization Properties of Full-length CrPHOT—Fast and slow components observed in the dark decay kinetics (Fig. 6) presumably represented LOV2 and LOV1 ($t_{1/2}$ = 15 and 50 s, respectively). Compared with the *Cr*PHOT LOV1+LOV2 fragment ($t_{1/2}$ = 17 and 200 s) (47), the

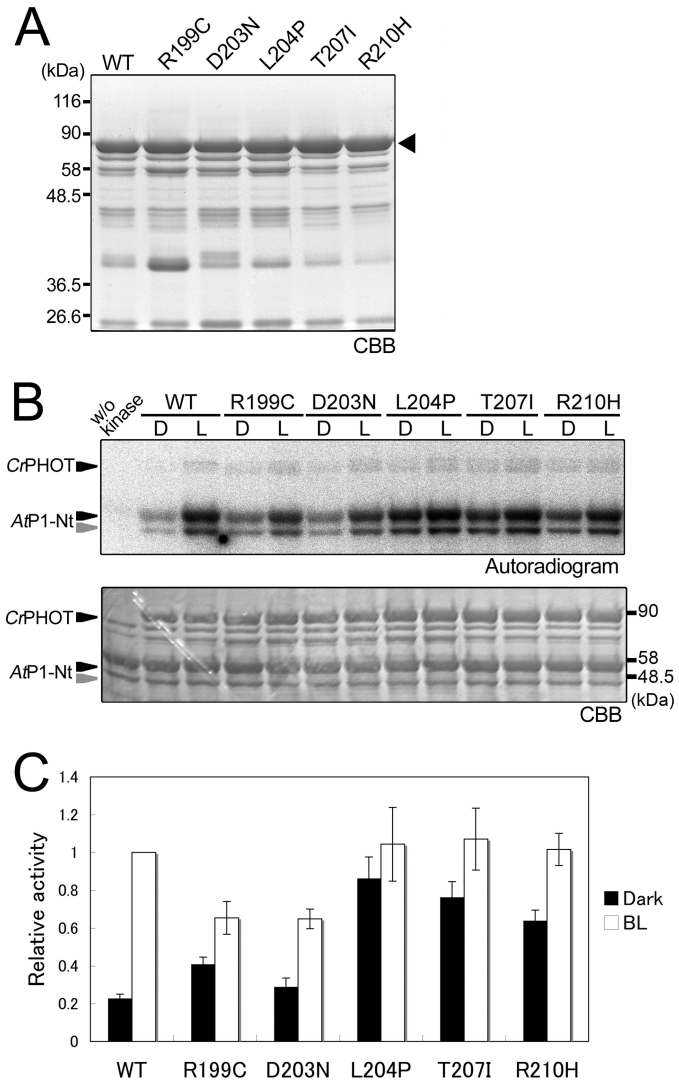

FIGURE 5. **Effects of *Cr*PHOT mutations on *in vitro* phosphorylation activity.** *A*, 10.0% SDS-polyacrylamide gel patterns of the mutant *Cr*PHOT proteins stained with CBB. The wild-type (*WT*) and the mutant *Cr*PHOT proteins were prepared as for Fig. 4*A*. The *triangle* indicates the position of the intact *Cr*PHOT. *B*, *in vitro* phosphorylation assay for the WT and mutant *Cr*PHOT samples. The reaction proceeded for 30 min under BL (100 μmol m^{-2} s^{-1}) or in the dark condition. Sample preparation and experimental procedures were the same as those for Fig. 4*B*. The *upper* and *lower panels* show the 10.0% SDS-polyacrylamide gel patterns visualized by autoradiography and CBB staining, respectively. *C*, quantification of the phosphorylation activity in the WT and the mutant *Cr*PHOT. An *in vitro* phosphorylation assay was performed as for *B*. Band intensities were quantified by a bioimaging analyzer and expressed relative to the maximal phosphorylation level in the WT under BL. The data represent the means of three independent experiments. *Error bars*, S.D.

slower component was four times faster in the full-length *Cr*PHOT. Hence, the presence of the C-terminal kinase domain might alter the photochemical kinetics of LOV1 as previously reported for *Arabidopsis* PHOT1 and PHOT2 (47).

The LOV1 domains of *Arabidopsis* PHOT1 and PHOT2 (43–45) and *Cr*PHOT (48) have been suggested to form a dimer and higher oligomers. However, size-exclusion chromatography in this study hinted that full-length *Cr*PHOT may exist as a monomer (apparent molecular mass of 123.7 kDa *versus* theoretical mass of 85.7 kDa) (supplemental Fig. S5). This possibility should be investigated further by other methods such as small angle x-ray scattering or crystallization analysis.

Mutations Outside LOV2 N-terminal Flanking Region—Prior to the present work, several amino acid substitutions in the N-terminal region of phototropins had been known to cause the pseudolit activation. Those include the ones in the Jα helix (V601E, A605E, and I608E in *Arabidopsis* PHOT1) (28) and the LOV2 core region (G513N in *Avena* PHOT1) (49). By contrast, such a mutation had not been known within the C-terminal region. In the present study, four novel mutations were found in addition to those clustered in the N-terminal LOV2 flanking region (see below).

Among them, L354P resides in the vicinity of Jα (Fig. 3*A* and supplemental Fig. S3). This is not surprising because several mutations are already known in this region to cause the pseudolit phenotype (see above). By contrast, Y39C in the LOV1 core region (Fig. 3*A* and supplemental Fig. S3) was somewhat unexpected because LOV1 is less important than LOV2 to regulate the kinase activity (18, 23, 24). However, LOV1 modifies the light sensitivity of PHOT2 (18). Hence, this mutation may affect the presumed LOV1/LOV2 or LOV1/kinase interaction to substantially increase the light sensitivity.

The N610S/T mutations in the activation loop of the kinase domain conferred the pseudolit phenotype (Fig. 3*A* and supplemental Fig. S3). Interestingly, the Asn^{610} residue is adjacent to Ser^{611}, which corresponds to the autophosphorylation site required for the activation of both PHOT1 and PHOT2 in *Arabidopsis* (13, 14) (supplemental Fig. S1). We constructed the N610A *Cr*PHOT to show that Ser^{610} and Thr^{610} but not Ala^{610} caused the pseudolit activation (supplemental Fig. S3). Hence, the newly introduced Ser/Thr^{610} might have acted as a secondary phosphorylation site to increase the kinase activity.

Involvement of N-terminal Flanking Region of LOV2 in Light-induced Signal Transduction—In our screening, we identified a novel mutational hot spot in the N-terminal flanking region of LOV2 (Arg^{199}-Arg^{210} in Fig. 3*A*). These mutations substantially reduced repression of the kinase activity by the N-terminal moiety in darkness (Figs. 3 and 5) without affecting the photochemical (Fig. 6) or multimerization properties of *Cr*PHOT (supplemental Fig. S5).

The crystal structure of LOV2 with N- and C-terminal flanking regions from *Avena* PHOT1 (residues Leu^{404}-Ala^{559} in *Avena* PHOT1) indicates that the N-terminal region (residues Leu^{404}-Arg^{414} in *Avena* PHOT1) is in the turn-helix-turn structure, in which the helix has been denoted as A′α (residues Thr^{407}-Arg^{410} in *Avena* PHOT1) (22). In this structure, A′α is packed against the surface of the β sheet of the LOV2 core domain to interact with the Jα helix (residues Asp^{522}-Ala^{543} in *Avena* PHOT1) in the C-terminal flanking region. Importantly, the light-induced structural rearrangements within the LOV2 core are associated with displacement of residues surrounding A′α (22). Hence, not only the C-terminal Jα helix but also the N-terminal flanking region are proposed to act as interfaces relaying the signal from the LOV2 core to the outside domain.

Our mutational analysis sheds new light on the biochemical function of the N-terminal flaking region of LOV2. The sequences in this region (Arg^{199}-Arg^{210}) are strikingly conserved among different phototropins (Fig. 3*B*). The alignment suggests that T207I and R210H reside within A′α

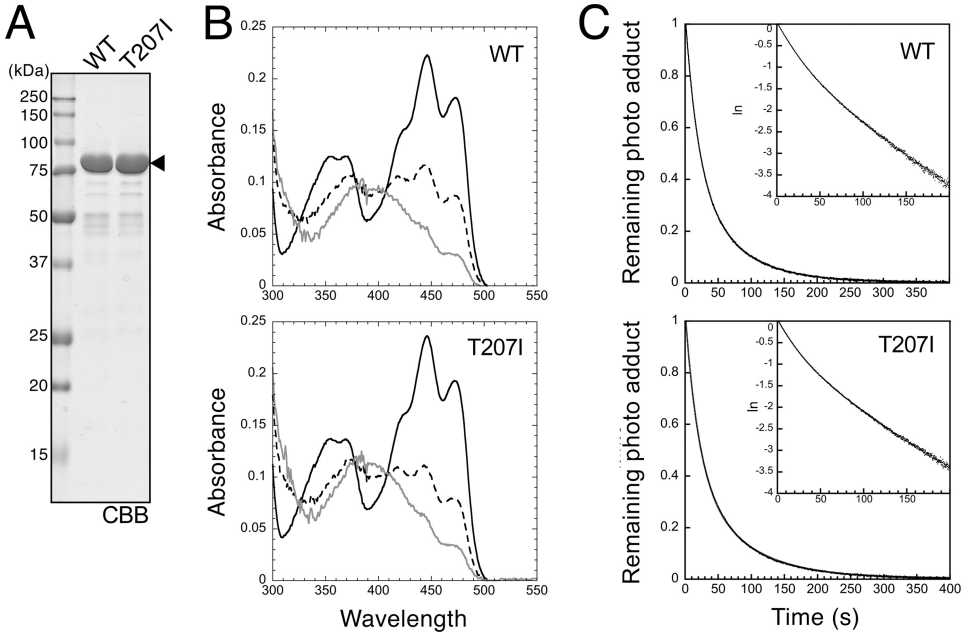

FIGURE 6. **Effects of the Thr^{207} mutation on photochemical properties.** *A*, 10.0% SDS-polyacrylamide gel pattern of full-length *Cr*PHOT samples stained with CBB. The sample was prepared using the same procedures as those for Fig. 5 and was further purified by anion-exchange chromatography. The *triangle* indicates the position of the intact *Cr*PHOT. *B*, absorption spectra of the WT and the T207I mutant *Cr*PHOT in darkness (*solid black lines*) and under BL irradiation at 50 μmol m^{-2} s^{-1} (*dashed black lines*) and 270 μmol m^{-2} s^{-1} (*gray lines*). The data represent the means of three measurements. *C*, kinetics of the reversion of the cysteinyl adduct state to the dark state monitored by the absorption at 450 nm. The samples were equilibrated under BL at 270 μmol m^{-2} s^{-1}, and the light was then tuned off at time 0. The remaining photoadduct level was calculated as $1 - (A_t - A_0)/(A_\infty - A_0)$, where A_t, A_∞, and A_0 are absorptions at 450 nm at time *t* in seconds, in darkness, and under BL, respectively. The logarithm of the remaining photoadduct level was plotted against *t* in the *inset*, indicating the fast and slow components of the reversion kinetics.

whereas L204P is in the loop upstream of A′α. Although the other three mutational sites, R199C, L202P, and D203N/G/V, are excluded from the above structural study, they are in close proximity on the primary structure. It should be noted here that a high degree of homology does not warrant similar phenotype in corresponding mutants of other phototropins. Indeed, *Arabidopsis* PHOT1 carrying T469I (corresponding to T207I in *Cr*PHOT) failed to show pseudolit activation (data not shown).

Hypothetical Extended A′α Helix May Play an Important Role for Intramolecular Signaling—Interestingly, a secondary structure prediction suggests that the A′α helix could be extended toward the N terminus to form a longer α helix (Arg^{199}-Arg^{210}), within which all the six mutational sites are mapped (supplemental Fig. S7*A*). Furthermore, the presumed α helix shows amphipathic character (supplemental Fig. S7*B*). The hydrophobic surface of this helix might then be packed against the hydrophobic LOV2 core. If this prediction is correct, the mutated residues residing in the polar surface of the helix (Arg^{199}, Asp^{203}, Thr^{207}, and Arg^{210}) might be directly involved in the physical interaction with other functional domains, such as the Jα helix and the C-terminal kinase. The existence of and a structural role for the predicted helix must be investigated in future studies.

Acknowledgments—We thank Prof. Masato Umeda and Dr. Utako Kato from Kyoto University for helpful discussions.

REFERENCES

1. Christie, J. M. (2007) Phototropin blue light receptors. *Annu. Rev. Plant Biol.* **58,** 21–45
2. Huala, E., Oeller, P. W., Liscum, E., Han, I. S., Larsen, E., and Briggs, W. R. (1997) *Arabidopsis* NPH1: a protein kinase with a putative redox-sensing domain. *Science* **278,** 2120–2123
3. Sakai, T., Kagawa, T., Kasahara, M., Swartz, T. E., Christie, J. M., Briggs, W. R., Wada, M., and Okada, K. (2001) *Arabidopsis* nph1 and npl1: blue light receptors that mediate both phototropism and chloroplast relocation. *Proc. Natl. Acad. Sci. U.S.A.* **98,** 6969–6974
4. Jarillo, J. A., Gabrys, H., Capel, J., Alonso, J. M., Ecker, J. R., and Cashmore, A. R. (2001) Phototropin-related NPL1 controls chloroplast relocation induced by blue light. *Nature* **410,** 952–954
5. Kagawa, T., Sakai, T., Suetsugu, N., Oikawa, K., Ishiguro, S., Kato, T., Tabata, S., Okada, K., and Wada, M. (2001) *Arabidopsis* NPL1: a phototropin homolog controlling the chloroplast high-light avoidance response. *Science* **291,** 2138–2141
6. Kinoshita, T., Doi, M., Suetsugu, N., Kagawa, T., Wada, M., and Shimazaki, K. (2001) Phot1 and phot2 mediate blue light regulation of stomatal opening. *Nature* **414,** 656–660
7. Sakamoto, K., and Briggs, W. R. (2002) Cellular and subcellular localization of phototropin 1. *Plant Cell* **14,** 1723–1735
8. Kozuka, T., Kong, S. G., Doi, M., Shimazaki, K., and Nagatani, A. (2011) Tissue-autonomous promotion of palisade cell development by phototropin 2 in *Arabidopsis*. *Plant Cell* **23,** 3684–3695
9. Huang, K., and Beck, C. F. (2003) Phototropin is the blue light receptor that controls multiple steps in the sexual life cycle of the green alga *Chlamydomonas reinhardtii*. *Proc. Natl. Acad. Sci. U.S.A.* **100,** 6269–6274
10. Im, C. S., Eberhard, S., Huang, K., Beck, C. F., and Grossman, A. R. (2006) Phototropin involvement in the expression of genes encoding chlorophyll and carotenoid biosynthesis enzymes and LHC apoproteins in *Chlamydomonas reinhardtii*. *Plant J.* **48,** 1–16
11. Onodera, A., Kong, S. G., Doi, M., Shimazaki, K., Christie, J., Mochizuki, N., and Nagatani, A. (2005) Phototropin from *Chlamydomonas reinhardtii* is functional in *Arabidopsis thaliana*. *Plant Cell Physiol.* **46,** 367–374
12. Galván-Ampudia, C. S., and Offringa, R. (2007) Plant evolution: AGC kinases tell the auxin tale. *Trends Plant Sci.* **12,** 541–547
13. Inoue, S., Kinoshita, T., Matsumoto, M., Nakayama, K. I., Doi, M., and

Shimazaki, K. (2008) Blue light-induced autophosphorylation of phototropin is a primary step for signaling. *Proc. Natl. Acad. Sci. U.S.A.* **105,** 5626–5631
14. Inoue, S., Matsushita, T., Tomokiyo, Y., Matsumoto, M., Nakayama, K. I., Kinoshita, T., and Shimazaki, K. (2011) Functional analyses of the activation loop of phototropin2 in *Arabidopsis*. *Plant Physiol.* **156,** 117–128
15. Christie, J. M., Yang, H., Richter, G. L., Sullivan, S., Thomson, C. E., Lin, J., Titapiwatanakun, B., Ennis, M., Kaiserli, E., Lee, O. R., Adamec, J., Peer, W. A., and Murphy, A. S. (2011) phot1 inhibition of ABCB19 primes lateral auxin fluxes in the shoot apex required for phototropism. *PLoS Biol.* **9,** e1001076
16. Crosson, S., and Moffat, K. (2001) Structure of a flavin-binding plant photoreceptor domain: insights into light-mediated signal transduction. *Proc. Natl. Acad. Sci. U.S.A.* **98,** 2995–3000
17. Kong, S. G., Kinoshita, T., Shimazaki, K., Mochizuki, N., Suzuki, T., and Nagatani, A. (2007) The C-terminal kinase fragment of *Arabidopsis* phototropin 2 triggers constitutive phototropin responses. *Plant J.* **51,** 862–873
18. Matsuoka, D., and Tokutomi, S. (2005) Blue light-regulated molecular switch of Ser/Thr kinase in phototropin. *Proc. Natl. Acad. Sci. U.S.A.* **102,** 13337–13342
19. Salomon, M., Christie, J. M., Knieb, E., Lempert, U., and Briggs, W. R. (2000) Photochemical and mutational analysis of the FMN-binding domains of the plant blue light receptor, phototropin. *Biochemistry* **39,** 9401–9410
20. Swartz, T. E., Corchnoy, S. B., Christie, J. M., Lewis, J. W., Szundi, I., Briggs, W. R., and Bogomolni, R. A. (2001) The photocycle of a flavin-binding domain of the blue light photoreceptor phototropin. *J. Biol. Chem.* **276,** 36493–36500
21. Crosson, S., and Moffat, K. (2002) Photoexcited structure of a plant photoreceptor domain reveals a light-driven molecular switch. *Plant Cell* **14,** 1067–1075
22. Halavaty, A. S., and Moffat, K. (2007) N- and C-terminal flanking regions modulate light-induced signal transduction in the LOV2 domain of the blue light sensor phototropin 1 from *Avena sativa*. *Biochemistry* **46,** 14001–14009
23. Christie, J. M., Swartz, T. E., Bogomolni, R. A., and Briggs, W. R. (2002) Phototropin LOV domains exhibit distinct roles in regulating photoreceptor function. *Plant J.* **32,** 205–219
24. Cho, H. Y., Tseng, T. S., Kaiserli, E., Sullivan, S., Christie, J. M., and Briggs, W. R. (2007) Physiological roles of the light, oxygen, or voltage domains of phototropin 1 and phototropin 2 in *Arabidopsis*. *Plant Physiol.* **143,** 517–529
25. Harper, S. M., Neil, L. C., and Gardner, K. H. (2003) Structural basis of a phototropin light switch. *Science* **301,** 1541–1544
26. Chen, E., Swartz, T. E., Bogomolni, R. A., and Kliger, D. S. (2007) A LOV story: the signaling state of the phot1 LOV2 photocycle involves chromophore-triggered protein structure relaxation, as probed by far-UV time-resolved optical rotatory dispersion spectroscopy. *Biochemistry* **46,** 4619–4624
27. Yamamoto, A., Iwata, T., Sato, Y., Matsuoka, D., Tokutomi, S., and Kandori, H. (2009) Light signal transduction pathway from flavin chromophore to the Jα helix of *Arabidopsis* phototropin1. *Biophys. J.* **96,** 2771–2778
28. Harper, S. M., Christie, J. M., and Gardner, K. H. (2004) Disruption of the LOV-Jα helix interaction activates phototropin kinase activity. *Biochemistry* **43,** 16184–16192
29. Takayama, Y., Nakasako, M., Okajima, K., Iwata, A., Kashojiya, S., Matsui, Y., and Tokutomi, S. (2011) Light-induced movement of the LOV2 domain in an Asp720Asn mutant LOV2-kinase fragment of *Arabidopsis* phototropin 2. *Biochemistry* **50,** 1174–1183
30. Christie, J. M., Corchnoy, S. B., Swartz, T. E., Hokenson, M., Han, I. S., Briggs, W. R., and Bogomolni, R. A. (2007) Steric interactions stabilize the signaling state of the LOV2 domain of phototropin 1. *Biochemistry* **46,** 9310–9319
31. Rose, M. D., Winston, F., and Hieter, P. (1990) *Methods in Yeast Genetics: A Laboratory Course Manual*, Cold Spring Harbor Laboratory, Cold Spring Harbor, NY
32. Nakano, K., Yamamoto, T., Kishimoto, T., Noji, T., and Tanaka, K. (2008) Protein kinases Fpk1p and Fpk2p are novel regulators of phospholipid asymmetry. *Mol. Biol. Cell* **19,** 1783–1797
33. Sikorski, R. S., and Hieter, P. (1989) A system of shuttle vectors and yeast host strains designed for efficient manipulation of DNA in *Saccharomyces cerevisiae*. *Genetics* **122,** 19–27
34. Kushnirov, V. V. (2000) Rapid and reliable protein extraction from yeast. *Yeast* **16,** 857–860
35. Okajima, K., Matsuoka, D., and Tokutomi, S. (2011) LOV2-linker-kinase phosphorylates LOV1-containing N-terminal polypeptide substrate via photoreaction of LOV2 in *Arabidopsis* phototropin1. *FEBS Lett.* **585,** 3391–3395
36. Saito, K., Fujimura-Kamada, K., Furuta, N., Kato, U., Umeda, M., and Tanaka, K. (2004) Cdc50p, a protein required for polarized growth, associates with the Drs2p P-type ATPase implicated in phospholipid translocation in *Saccharomyces cerevisiae*. *Mol. Biol. Cell* **15,** 3418–3432
37. Chen, S., Wang, J., Muthusamy, B. P., Liu, K., Zare, S., Andersen, R. J., and Graham, T. R. (2006) Roles for the Drs2p-Cdc50p complex in protein transport and phosphatidylserine asymmetry of the yeast plasma membrane. *Traffic* **7,** 1503–1517
38. Pomorski, T., Lombardi, R., Riezman, H., Devaux, P. F., van Meer, G., and Holthuis, J. C. (2003) Drs2p-related P-type ATPases Dnf1p and Dnf2p are required for phospholipid translocation across the yeast plasma membrane and serve a role in endocytosis. *Mol. Biol. Cell* **14,** 1240–1254
39. Kong, S. G., Suzuki, T., Tamura, K., Mochizuki, N., Hara-Nishimura, I., and Nagatani, A. (2006) Blue light-induced association of phototropin 2 with the Golgi apparatus. *Plant J.* **45,** 994–1005
40. Jones, M. A., and Christie, J. M. (2008) Phototropin receptor kinase activation by blue light. *Plant Signal. Behav.* **3,** 44–46
41. Jones, M. A., Feeney, K. A., Kelly, S. M., and Christie, J. M. (2007) Mutational analysis of phototropin 1 provides insights into the mechanism underlying LOV2 signal transmission. *J. Biol. Chem.* **282,** 6405–6414
42. Guo, H., Kottke, T., Hegemann, P., and Dick, B. (2005) The phot LOV2 domain and its interaction with LOV1. *Biophys. J.* **89,** 402–412
43. Nakasako, M., Iwata, T., Matsuoka, D., and Tokutomi, S. (2004) Light-induced structural changes of LOV domain-containing polypeptides from *Arabidopsis* phototropin 1 and 2 studied by small-angle x-ray scattering. *Biochemistry* **43,** 14881–14890
44. Salomon, M., Lempert, U., and Rüdiger, W. (2004) Dimerization of the plant photoreceptor phototropin is probably mediated by the LOV1 domain. *FEBS Lett.* **572,** 8–10
45. Nakasako, M., Zikihara, K., Matsuoka, D., Katsura, H., and Tokutomi, S. (2008) Structural basis of the LOV1 dimerization of *Arabidopsis* phototropins 1 and 2. *J. Mol. Biol.* **381,** 718–733
46. Pfeifer, A., Mathes, T., Lu, Y., Hegemann, P., and Kottke, T. (2010) Blue light induces global and localized conformational changes in the kinase domain of full-length phototropin. *Biochemistry* **49,** 1024–1032
47. Kasahara, M., Swartz, T. E., Olney, M. A., Onodera, A., Mochizuki, N., Fukuzawa, H., Asamizu, E., Tabata, S., Kanegae, H., Takano, M., Christie, J. M., Nagatani, A., and Briggs, W. R. (2002) Photochemical properties of the flavin mononucleotide-binding domains of the phototropins from *Arabidopsis*, rice, and *Chlamydomonas reinhardtii*. *Plant Physiol.* **129,** 762–773
48. Kutta, R. J., Hofinger, E. S., Preuss, H., Bernhardt, G., and Dick, B. (2008) Blue light induced interaction of LOV domains from *Chlamydomonas reinhardtii*. *ChemBioChem* **9,** 1931–1938
49. Nash, A. I., Ko, W. H., Harper, S. M., and Gardner, K. H. (2008) A conserved glutamine plays a central role in LOV domain signal transmission and its duration. *Biochemistry* **47,** 13842–13849